Competition between dynamic and structural disorder in a doped triangular antiferromagnet $RbFe(MoO_4)_2$

IOP Conf. Series: Journal of Physics: Conf. Series **969** (2018) 012115 doi:10.1088/1742-6596/969/1/012115

Competition between dynamic and structural disorder in a doped triangular antiferromagnet $RbFe(MoO_4)_2$

A I Smirnov[1,2], T A Soldatov[1,3], O A Petrenko[4], A Takata[5], T Kida[5], M Hagiwara[5], M E Zhitomirsky[6] and A Ya Shapiro[7]

[1] P.L. Kapitza Institute for Physical Problems RAS, Moscow 119334, Russia
[2] Higher School of Economics, 101000 Moscow, Russia
[3] Moscow Institute for Physics and Technology, Dolgoprudny 141700, Russia
[4] Department of Physics, University of Warwick, Coventry CV4 7AL, United Kingdom
[5] Center of Advanced High Magnetic Field Science (AHMF), Graduate School of Science, Osaka University, Osaka 560-0043, Japan
[6] Service de Physique Statistique, Magnetisme et Supraconductivite, UMR-E9001 CEA-INAC/UJF, 17 rue des Martyrs, Grenoble 38054, France
[7] A. V. Shubnikov Institute for Crystallography RAS, Moscow 119333, Russia

E-mail: smirnov@kapitza.ras.ru

Abstract. Magnetisation measurements and electron spin resonance (ESR) spectra of a doped quasi two dimensional (2D) antiferromagnet on a triangular lattice $Rb_{1-x}K_xFe(MoO_4)_2$ reveal a crucial change of the ground state spin configuration and a disappearance of a characteristic 1/3-magnetisation plateau at $x = 0.15$. According to theory for triangular antiferromagnets with a weak random modulation of the exchange bonds, this is a result of the competition between the structural and dynamic disorders. The dynamic zero-point or thermal fluctuations are known to lift the degeneracy of the mean field ground state of a triangular antiferromagnet and cause the spin configuration to be the most collinear, while the static disorder provides another selection of the ground state, with the least collinear structure. Low-level doping ($x \leq 0.15$) was found to decrease the Néel temperature and saturation field by only few percent, while the magnetisation plateau disappears completely and the spin configuration is drastically changed. ESR spectra confirm an impurity-induced change of the so-called Y-type structure to an inverted Y-structure for $x = 0.15$. For $x = 0.075$ the intermediate regime with the decrease of width and weakening of flattening of 1/3-plateau was found.

1. Introduction

Triangular lattice antiferromagnets (TLAF) provide challenges in contemporary magnetism due to the frustration of the exchange interaction and unusual magnetic phases, stabilised by fluctuations (for reviews, see, *e.g.*, Refs. [1–3]). The ground state of a TLAF in a magnetic field is strongly degenerate in a mean field approximation. The selection of the ground state is made through the so-called order-by-disorder mechanism, implying that thermal and quantum spin fluctuations lift the degeneracy of a classical ground state. A key feature of TLAF is the 1/3-magnetisation plateau with the collinear up-up-down (*uud*) spin structure stabilised by fluctuations [4–6]. This phase has been experimentally observed in several TLAFs [7–9].

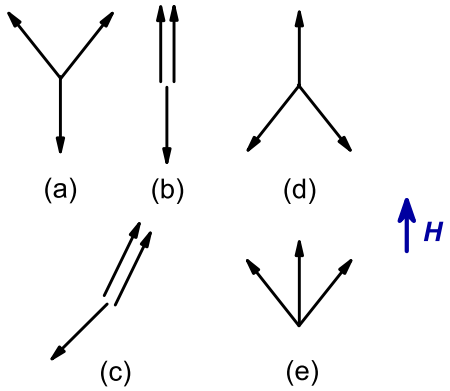

Figure 1. Spin structures stabilised in the pure TLAF in an applied field: (a) the Y-state, (b) the *uud*-state, (c) the 2:1 state. Spin structures of a planar TLAF with structural disorder: (d) inverted Y-state and (e) the fan state.

A recent theory [10, 11] predicted that the 1/3-plateau may be suppressed in the presence of a weak random modulation of the exchange bonds, which should lift the degeneracy. Apart from cancelling the plateau, a modification of the low- and high-field spin configuration is expected even at a very low doping: in low fields, the three-sublattice Y-structure should be changed for the inverted Y-state, while in high fields, the 2:1 structure should be replaced by the umbrella-type structure for a Heisenberg TLAF or by the fan-type structure for an XY TLAF, see the configuration sketches in Fig. 1. Formally, the impact of structural disorder on the degeneracy lifting in frustrated magnets may be represented by an effective biquadratic exchange with a positive sign [10–14]. The fluctuation contribution to the free energy is presented by a negative biquadratic term.

$RbFe(MoO_4)_2$ is a model TLAF formed by layers of magnetic Fe^{3+} ions with a semiclassical $S = 5/2$ spin. At $T_N = 4.1$ K it exhibits a spin ordering within the layers with the three magnetic sublattices 120° apart, while the spin correlations in the adjacent layers correspond to an incommensurate structure, with the angle of 165° between the neighbouring spins [15]. The system has an easy-plane magnetic anisotropy with the plane parallel to layers and demonstrates a 1/3-magnetisation plateau for $H \perp c$ (the c axis is perpendicular to the magnetic layers) [16,17]. The $H-T$ phase diagram corresponds well to the XY-TLAFM [16]. To perform a weak random modulation of exchange bonds we partially substitute Rb for K, disturbing the triangular layers by replacing nonmagnetic ions in the interlayer space.

In this paper we describe a study of K-doped samples $Rb_{1-x}K_xFe(MoO_4)_2$ with $x = 0, 0.075$ and 0.15 by means of electron spin resonance (ESR) spectroscopy and magnetisation measurements for the in-plane magnetic field. The mean-field parameters of the doped samples (the Néel temperature T_N, the saturation field H_{sat} and the gap of antiferromagnetic resonance Δ) were measured in a set of preliminary experiments, they showed a monotonic decrease by only a few percent for this range of impurity concentration, whereas the pulsed-field magnetisation curves demonstrated a complete disappearance of the plateau upon doping (the data are published elsewhere [18]). We report here the steady-field magnetisation curves, which have a higher signal to noise ratio compared to the pulsed field measurements and also correspond to a truly equilibrium regime. These data, as well as the ESR spectra, are compared for the pure sample, the intermediately doped sample ($x = 0.075$), and the sample with $x = 0.15$, the last is demonstrating a complete cancellation of the plateau and a change of the ground state.

2. Experimental methods

The crystals of $Rb_{1-x}K_xFe(MoO_4)_2$ were prepared as previously described [8]. The K content x was determined by means of energy-dispersive X-ray spectroscopy.

The ESR signal is recorded as the field dependence of the microwave power transmitted through the resonator with the sample inside. A set of resonator-type spectrometers for the

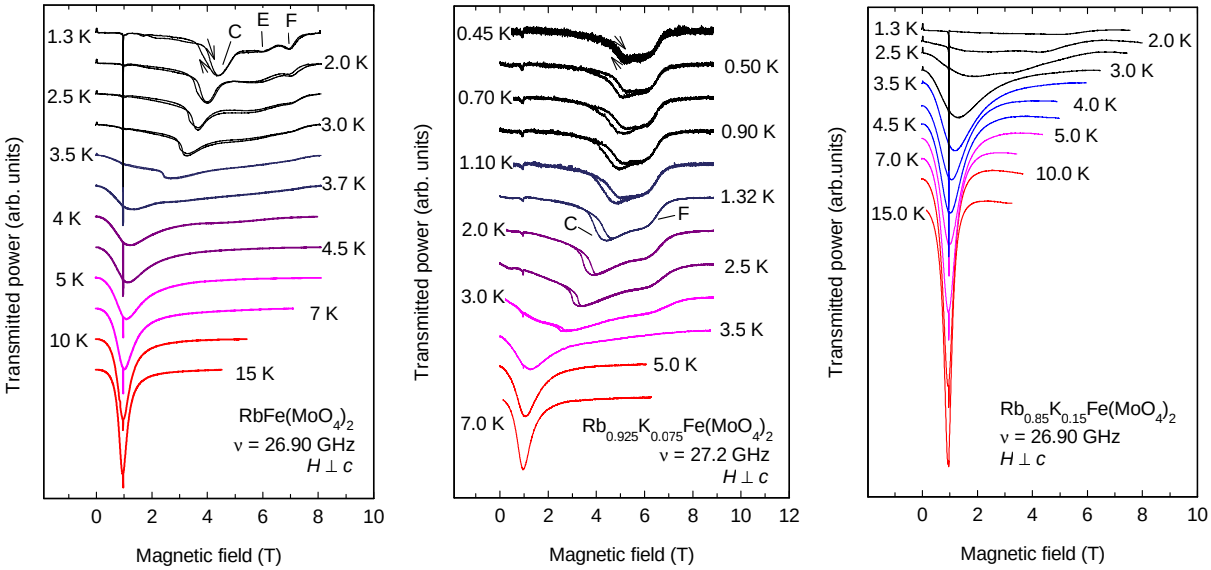

Figure 2. Temperature evolution of the ESR absorption curve for $x = 0$ (left panel), $x = 0.075$ (middle), and $x = 0.15$ (right panel).

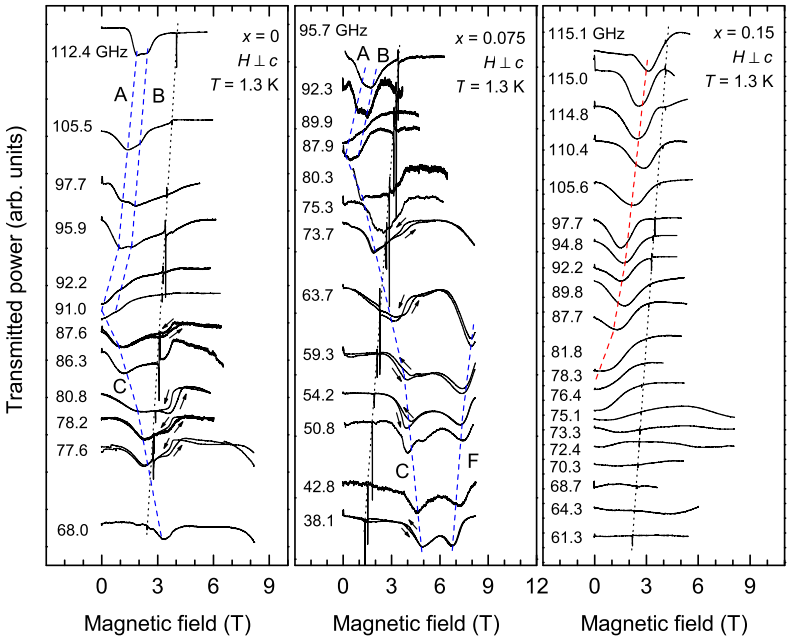

Figure 3. Normalised ESR absorption curves for the in-plane magnetic field for $Rb_{1-x}K_xFe(MoO_4)_2$ samples with $x = 0$, 0.075 and 0.15 for different frequencies. Dashed lines are a guide to the eye. The narrow ESR line is a DPPH label with $g = 2.00$. The gain is normalised to the intensity of the paramagnetic resonance signal at $T = 10$ K.

frequency range 25 - 120 GHz, combined with the ^{4}He and ^{3}He cryostats and superconducting solenoids was used. Frequency-field dependencies for the in-plane orientation of the magnetic field and temperature evolution of the ESR spectra were obtained. Magnetisation curves were measured using both a vibrating sample magnetometer and a pulsed field magnet.

3. Experimental results

As described in [8], on cooling the sample the ESR line broadens below 10 K. After passing through the Néel point, the ESR line shifts from the paramagnetic resonance position and again becomes narrow, exhibiting a splitting at some frequencies into a few antiferromagnetic

resonance modes. A nonresonant change in the microwave susceptibility is also observed near a critical field with an abrupt change in the mutual orientation of spins in adjacent layers (4 T in the pure sample). This transition is accompanied by a hysteresis, marked by arrows denoting up and down field-sweep records in Figs. 2 and 3. The typical temperature evolution of an ESR line is presented in Fig. 2 for $x = 0, 0.075$ and 0.15. For different frequencies from the range 25-120 GHz, the field dependencies of the microwave transmission at $T = 1.3$ K for $x = 0, 0.075$ and 0.15 are shown in Fig. 3 for the in-plane magnetic field. The corresponding frequency-field dependencies of the spin-resonance modes are reconstructed in Fig. 4.

In correspondence with earlier observations [8], the ESR spectrum of a pure sample has an energy gap $\Delta_0 \simeq 90$ GHz and in low fields consists mainly of two branches. The frequency of the first branch rises with field, while the frequency of the second branch decreases. The ascending branch is split into two close branches (A) and (B) because of the interplane interaction [8]. The descending branch (C) goes to almost zero frequency near the lower boundary of the plateau. Another branch (F) at a frequency much lower than Δ_0 arises at the upper boundary of the plateau. Thus the resonance fields of modes C and F observed at a low frequency of about 25 GHz mark the boundaries of the plateau. Another mode (D) appears near the onset of the plateau at a frequency higher than that of mode C. Mode E in the middle of the plateau

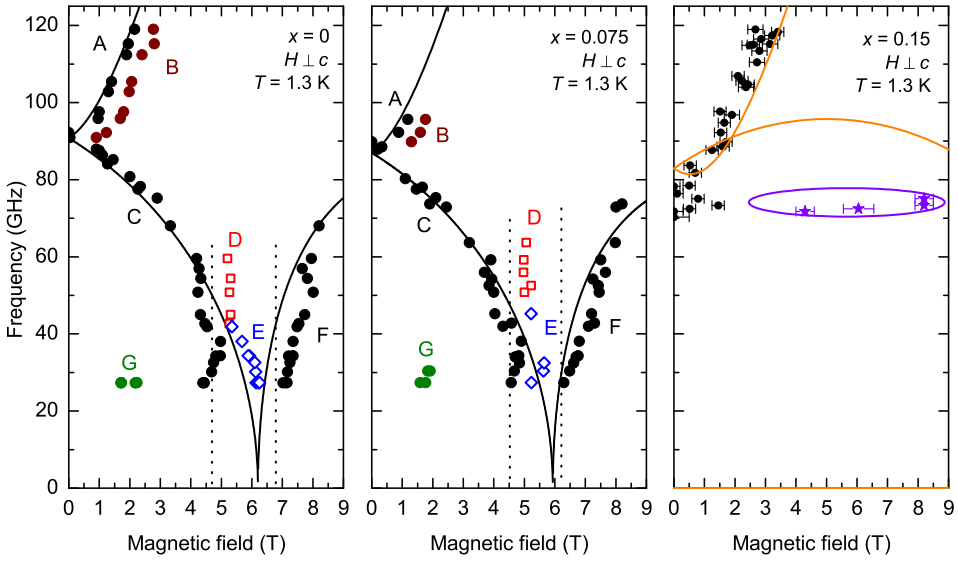

Figure 4. Frequency-field diagrams for the $Rb_{1-x}K_xFe(MoO_4)_2$ samples with different doping concentration x. The magnetic field is applied parallel to the magnetic layers. For $x = 0$ and 0.075, the solid lines represent theoretical calculations for the Y-type structure with parameters $J = 1.1J_0$ and $J = 1.03J_0$ respectively, while for the $x = 0.15$ sample the calculations are for the inverted Y state with $J = 0.9J_0$. Vertical dotted lines indicate 1/3-plateau boundaries evaluated from the dM/dH curves (see Fig. 5). The ellipse covers a wide area of a weak absorption.

and the above mentioned modes A-D and F are all in accord with the theory [6] and previous experiments [8]. In addition, a weakly-absorbing mode (G) near 30 GHz exists due to a splitting of the zero-frequency mode [8].

The 27 GHz ESR records, which are sensitive to the plateau boundaries at the critical fields H_{c1} and H_{c2}, are shown in Fig. 2. These data demonstrate that the features associated with the plateau in the ESR spectrum for the $x = 0.075$ sample are weaker, but still present, while for the $x = 0.15$ sample there is trace of the no plateau in the low temperature record. The intensities of

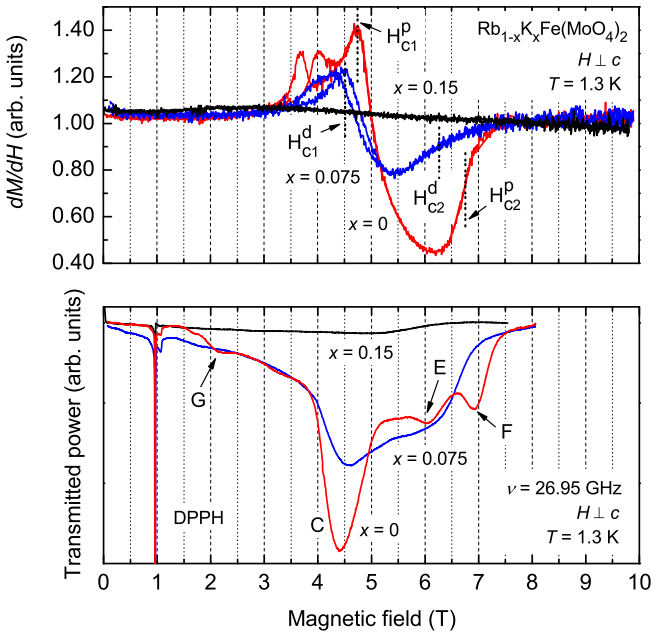

Figure 5. Upper panel: dM/dH curves for $Rb_{1-x}K_xFe(MoO_4)_2$ samples with $x = 0$ and 0.075 measured in a static field by a vibrating sample magnetometer at $T = 1.3$ K. Lower panel: normalised ESR absorption curves for $x = 0$ and 0.075 samples. Resonance modes C, E, F, G are marked for the $x = 0$ sample in accordance with notation in Figs. 3 and 4.

resonance modes C and F are smaller in the intermediately doped sample ($x = 0.075$), and the width of the plateau, marked by these modes is reduced as compared to the pure sample. Figure 5 shows ESR response for all three concentrations at a low temperature $T = 1.3$ K, compared with dM/dH curves of these samples. A long continuous drop of the dM/dH curve marks the plateau range. We see that for $x = 0.075$ the drop of dM/dH is much smaller, than for a pure sample, and for $x = 0.15$ the plateau disappears completely. At the same time the dM/dH curve of the $x = 0.075$ sample marks distinctly the lower critical field H_{c1}, while the upper field H_{c2} is smeared. We estimate the upper boundary of the plateau as the field where the change of dM/dH reaches 1/2 of the total change during the return of dM/dH to its nominal value. The estimated values of the critical fields both for a pure sample $H^{\rm p}_{c1,2}$ and for $x = 0.075$ sample $H^{\rm d}_{c1,2}$ correspond well to positions of ESR modes C and F. Both the drop of dM/dH and ESR intensity of modes C and F demonstrate a vanishing in the $x = 0.075$ doped sample compared to a pure sample. This drop is much stronger than the diminishing of $T_{\rm N}$ or H_{sat}. The 27 GHz ESR response of the $x = 0.15$ sample is practically absent, as shown in Fig. 5, analogous to the absence of the drop of dM/dH. Thus, both the ESR signals and $M(H)$ curves of the $x = 0.15$ sample reveal the disappearance of the plateau, while the medium doped sample has a plateau reduced both in width and in flatness.

4. Disscussion

The ESR spectrum for the $x = 0.15$ doped sample demonstrates significant modifications in the entire range of applied magnetic fields. The descending ESR branch observed in the pure sample either completely disappears or transforms to a field-independent mode (see Figs. 3 and 4). This indicates a drastic change of the magnetic ground state with doping, and in particular, a full suppression of the ESR modes in the field range of the 1/3-magnetisation plateau and the complete absence of the descending branch C. At the same time, the frequency-field diagram for an intermediately doped sample indicates a narrowing of the plateau as well as a reduction of the energy gap by about of 5 percent, but remains broadly similar to that of a pure sample. We propose, that the crucial change of the ESR spectrum of the $x = 0.15$ sample is due to a change in the ground state spin configuration. To check this conjecture we have calculated the

frequency-field dependencies using two models of the ground state, the Y-phase of a TLAF and the inverted Y-phase. The details of the theory of the ESR frequencies for these different spin structure models will be published elsewhere [18]. The results of the calculation are presented in Fig. 4 as solid lines. Calculations for the Y-type spin structure are shown in the left and middle panels in Fig. 4, and for the inverted Y-structure, in the right panel. The parameters used for the calculations for the pure compound are the main intraplane exchange integral, J_0 and the single-ion anisotropy constant, D_0. For the pure compound the parameters obtained from neutron scattering experiments [19] are: $J_0 = 0.086$ meV, $D_0 = 0.027$ meV. For fitting the theoretical frequency-field dependencies we used the parameters $J = 1.1J_0$ for $x = 0$, $J = 1.03J_0$ for $x = 0.075$ samples, and $J = 0.9J_0$ for $x = 0.15$ samples (the anisotropy term is kept equal to the D_0 of the pure sample). The decrease of the exchange interaction with doping agrees well with the observed decrease of H_{sat} and $T_{\rm N}$. From a comparison of the experimental data with the theoretical frequency-field dependencies we conclude, that the possible change of the ground state, induced by doping is from the Y- to inverted Y-phase, as predicted by [10, 11].

5. Conclusions

Measurements of the magnetisation versus field and the ESR spectra confirm the theoretical predictions that in a triangular antiferromagnet the 1/3 magnetisation plateau is dramatically suppressed by a moderate random modulation of the intraplane exchange interaction. The variation of magnetic resonance spectrum on doping, including the disappearance of the descending branch for $x = 0.15$, verifies the stabilisation of an inverted Y-state instead of Y structure.

Acknowledgments

The work is supported by the Russian Foundation for Fundamental research, grant N 15-02-05918, Russian Science Foundation, grant N 17-1201505, by the Program of the Presidium of Russian Academy of Sciences, and by International Joint Research Promotion Program (short term) in Osaka University.

References

[1] Collins M F and Petrenko O A 1997 *Can. J. Phys.* **75** 605
[2] Balents L 2010 *Nature* **464** 199
[3] Starykh O A 2015 *Rep. Prog. Phys.* **78** 052502
[4] Lee D H, Joannopoulos J D, Negele J W and Landau D P 1984 *Phys. Rev. Lett.* **52** 433
[5] Kawamura H and Miyashita S 1985 *J. Phys. Soc. Jpn.* **54** 4530
[6] Chubukov A V and Golosov D I 1991 *J. Phys.: Condens. Mat.* **3** 69
[7] Inami T, Ajiro Y and Goto T 1996 *J. Phys. Soc. Jpn.* **65** 2374
[8] Svistov L E, Smirnov A I, Prozorova L A, Petrenko O A, Demianets L N and Shapiro A Ya 2003 *Phys. Rev. B* **67** 094434
[9] Shirata Yu, Tanaka H, Matsuo A and Kindo K 2012 *Phys. Rev. Lett.* **108** 057205
[10] Maryasin V S and Zhitomirsky M E 2013 *Phys. Rev. Lett.* **111** 247201
[11] Maryasin V S and Zhitomirsky M E 2015 *J. Phys.: Confer. Ser.* **592** 012112
[12] Henley C L 1989 *Phys. Rev. Lett.* **62** 2056
[13] Long M W 1989 *J. Phys.: Condens. Mat.* **1** 2857
[14] Fyodorov Y V and Shender E F 1991 *J. Phys. Condens. Mat.* **3** 9123
[15] Kenzelman M, Lawes G, Harris A B, Gasparovic G, Broholm C, Ramirez A P, Jorge G A, Jaime M, Park S, Huang Q, Shapiro A Ya, Demianets L N 2007 *Phys. Rev. Lett.* **98**, 267205
[16] Svistov L E, Smirnov A I, Prozorova L A, Petrenko O A, Micheler A, Buttgen N, Shapiro A Ya and Demianets L N 2006 *Phys. Rev. B* **74** 024412
[17] Smirnov A I, Yashiro H, Kimura S, Hagiwara M, Narumi Y, Kindo K, Kikkawa A, Katsumata K, Shapiro A Ya and Demianets L N 2007 *Phys. Rev. B* **75** 134412
[18] Smirnov A I, Soldatov T A, Petrenko O A, Takata A, Kida T, Hagiwara M, Zhitomirsky M E, and Shapiro A Ya 2017 *Phys. Rev. Lett.* **119**, 047204

[19] White J S, Niedermayer Ch, Gasparovic G, Broholm C, Park J M S, Shapiro A Ya, Demianets L N and Kenzelmann M 2013 *Phys. Rev. B* **88** 060409